

# Photoluminescence of the Beryllium Acceptor at the Centre of Quantum Wells\*

Zheng Weimin<sup>†</sup>, Li Sumei, Lü Yingbo, Wang Aifang, and Wu Ailing

(School of Space Science and Physics, Shandong University at Weihai, Weihai 264209, China)

**Abstract:** We report photoluminescence studies of internal transitions of shallow Be acceptors in bulk GaAs and a series of  $\delta$ -doped GaAs/AlAs multiple quantum well samples with well width ranging from 3 to 20nm. A series of Be  $\delta$ -doped GaAs/AlAs multiple-quantum wells with the doping at the well center and a single epilayer of GaAs uniformly Be doped were grown by molecular beam epitaxy. The photoluminescence spectra were measured at 4, 20, 40, 80, and 120K, respectively. A two-hole transition of the acceptor-bound exciton from the ground state,  $1S_{3/2}(\Gamma_6)$ , to the first-excited state,  $2S_{3/2}(\Gamma_6)$ , has been clearly observed. A variational principle is presented to obtain the  $2s-1s$  transition energies of quantum confined Be acceptors as a function of the well width under the single-band effective mass and envelop function approximations. It is found that the acceptor transition energy increases with decreasing quantum-well width, and the experimental results agree well with the theoretical calculation.

**Key words:** quantum confined acceptors;  $\delta$ -doped; multiple quantum wells; photoluminescence

**PACC:** 7320D; 7855E; 7155F

**CLC number:** TN304.2+3

**Document code:** A

**Article ID:** 0253-4177(2008)11-2115-06

## 1 Introduction

Impurity states in quantum wells have been extensively studied because of their potential in optoelectronic applications, such as low input power sources of terahertz detectors ( $1\sim 10\text{THz}$ ) and emitters<sup>[1-4]</sup>. In principle either donors or acceptors could be used to form the energy levels of a device. However, in practice the greater binding energy of the acceptors makes them attractive candidates as they can have their transition energies moved over a wider range by varying the quantum confined environment of the impurity. In addition, the transition energy could exceed the longitudinal optical phonon energy, thus significantly reducing this non-radiative loss mechanism.

In the GaAs/Ga<sub>1-x</sub>Al<sub>x</sub>As quantum-well system, beryllium is a commonly used acceptor; beryllium is relatively stable with respect to diffusion and has a binding energy of 28.0meV in bulk<sup>[5]</sup>. The use of  $\delta$  doping avoids the extension of the impurity energy levels resulting from a distribution of the dopant atoms along the growth direction of the quantum wells. The first calculation on the Be acceptor states in GaAs/Al<sub>x</sub>Ga<sub>1-x</sub>As quantum wells incorporating with a complicated valence-band structure was performed by Masselink *et al.*<sup>[6]</sup>. Experimentally, resonant Ra-

man scattering<sup>[7]</sup> and far-infrared absorption<sup>[8,9]</sup> have been used to investigate the transitions of shallow acceptor states. Subsequently, Holtz *et al.* reported measurements on the transitions from the ground state to excited states via two-hole transitions and Raman scattering for GaAs/Al<sub>x</sub>Ga<sub>1-x</sub>As quantum wells with well thicknesses in the range  $5\sim 13.8\text{nm}$ <sup>[10,11]</sup>. However, for GaAs/AlAs multiple-quantum wells with Be acceptors doped at the well center, there have been few reports of either experimental or theoretical work. This system is of special interest as it represents the maximum possible confinement for the acceptor states in the valence band. In this paper, we measure photoluminescence (PL) spectra at various temperatures for a series of GaAs/AlAs multiple-quantum wells with Be  $\delta$ -doped at the well center and a single epilayer of GaAs uniformly Be doped (GaAs:Be). The transitions of the shallow acceptor states have been investigated by observing the two-hole transition of the acceptor-bound exciton. A variational principle is presented to obtain the  $2s-1s$  transition energies of quantum confined Be acceptors as a function of the well width.

## 2 Experiment and results

The samples were grown by molecular-beam epi-

\* Project supported by the National Natural Science Foundation of China (No.60776044) and the Natural Science Foundation of Shandong Province (No.2006ZRA10001)

<sup>†</sup> Corresponding author. Email: wmzheng@sdu.edu.cn

Received 3 June 2008, revised manuscript received 15 July 2008

Table 1 Characteristics of the samples studied; the repeated period, the quantum-well width ( $L$ ), the  $\delta$ -doping concentration ( $P$ ) and the growth temperature of the epitaxial layer ( $T$ )

Sample	Period	$L/\text{nm}$	$P/\text{cm}^{-2}$	$T/^\circ\text{C}$
1	400	3	$2 \times 10^{10}$	550
2	200	10	$5 \times 10^{10}$	550
3	50	15	$2.5 \times 10^{12}$	540
4	40	20	$2.5 \times 10^{12}$	540
5	a single $5\mu\text{m}$ -thick epilayer (GaAs:Be)		$2 \times 10^{16}$	550

taxy on semi-insulating (100) GaAs substrates in a VG V80 H reactor equipped with all solid sources. The growth of the layers was performed using the stoichiometric low-temperature growth technique<sup>[12]</sup>. This ensures high quality optical materials even at relatively low growth temperatures. Under these conditions, the quantum-well structures were grown at  $550^\circ\text{C}$  without interruptions at the quantum well interfaces, ensuring negligible diffusion of the Be within the layers. Prior to the growth of the multiple-quantum wells, a 300nm GaAs buffer layer was grown. Each of the multiple quantum well structures contains the same 5nm wide AlAs barrier, while every GaAs well layer is  $\delta$ -doped at the well center with Be acceptor atoms. The doping level and the main characteristics of each sample are summarized in Table 1.

Photoluminescence (PL) experiments were performed from liquid helium to room temperature using a Renishaw Raman microscope system. The samples were mounted on a cold finger of a continuous flow helium cryostat. The optical excitation for the PL experiments was provided by an argon-ion laser (514.5nm). The laser beam was focused onto a sample, and the light returning back from the sample was collected and passed into the spectrometer for analysis. The excitation was typically 5mW with a spot size of about  $2\mu\text{m}$ . The spectra resolution of the system is  $200\mu\text{eV}$ .

In bulk GaAs, the top of the valence band was characterized by the total angular momentum  $J = 3/2$  and it was thus four-fold degenerate (with  $m_j = \pm 1/2, \pm 3/2$ ) at the  $\Gamma$  point ( $k = 0$ ). Away from  $k = 0$ , this degeneracy was partially lifted by the spin-orbit interaction into a doubly degenerate heavy-hole state, with  $m_j = \pm 3/2$  of  $\Gamma_6$  symmetry, and a doubly-degenerate light-hole state with  $m_j = \pm 1/2$  of  $\Gamma_7$  symmetry. The lowest Be acceptor states in bulk GaAs are identified as  $1s_{3/2}\Gamma_8$ ,  $2p_{3/2}\Gamma_8$ ,  $2s_{3/2}\Gamma_8$ ,  $2p_{5/2}\Gamma_8$ ,  $2p_{5/2}\Gamma_7$ , and  $2p_{1/2}\Gamma_6$ . When Be acceptors are introduced into the GaAs/ $\text{Al}_x\text{Ga}_{1-x}\text{As}$  quantum wells from the bulk, the degeneracy of the valence band is lifted at the  $\Gamma$  point due to the quantum well potential, reducing the point group symmetry from  $T_d$  to  $D_{2d}$ . There-

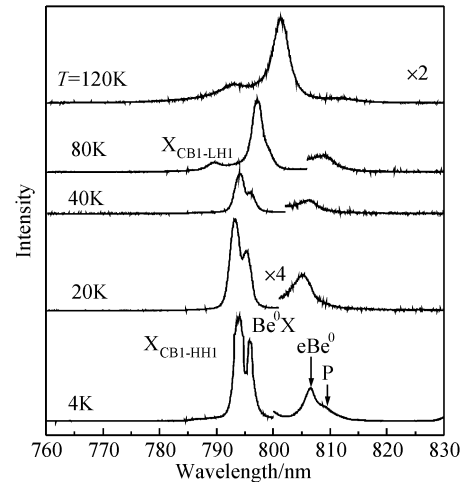


Fig.1 Series of PL spectra of the sample 2 ( $L = 10\text{nm}$ ) at different measuring temperatures with the excitation power of the 514.5nm radiation, showing the  $X_{\text{CBI-LHI}}$ ,  $X_{\text{CBI-HHI}}$ ,  $\text{Be}^0\text{X}$ ,  $e\text{Be}^0$ , and P peaks. The excitation was typically 5mW.

fore, the  $1s_{3/2}\Gamma_8$  acceptor ground state and  $2p_{3/2}\Gamma_8$ ,  $2s_{3/2}\Gamma_8$  and  $2p_{5/2}\Gamma_8$  excited states are split accordingly into  $1s_{3/2}(\Gamma_6 + \Gamma_7)$  and  $2p_{3/2}(\Gamma_6 + \Gamma_7)$ ,  $2s_{3/2}(\Gamma_6 + \Gamma_7)$ ,  $2p_{5/2}(\Gamma_6 + \Gamma_7)$ , respectively<sup>[8]</sup>.

The PL spectra with above-band gap excitation have been measured at the various temperatures for the samples in Table 1. Figures 1 and 2 shows the PL spectra at 4, 20, 40, 80, and 120K for the two samples having well widths of 10nm (sample 2) and 3nm (sample 1), respectively. Sample 1 represents the limiting case for Be  $\delta$  doping at the centre of a quantum well. The well width of sample 2 enables an easier optical analysis for quantum well extrinsic transitions that do not overlap with the near-bandgap radiative emissions of bulk GaAs. Some differences can be observed in the low-temperature excitonic signals. In Fig. 1, for sample 2 with a quantum-well width of 10nm, three strong peaks are clearly resolved at 4K, with positions located at 794, 795.88, and 806.26nm, respectively. The first at 794nm is the strongest peak and attributed unambiguously to the transition of a heavy free exciton ( $X_{\text{CBI-HHI}}$ ). Its maximum correlates with the temperature dependence of the GaAs bandgap and it does not exhibit any blue shift when the temperature increases. The second at 795.88nm originates from the exciton recombination bound to the neutral beryllium acceptor ( $\text{Be}^0\text{X}$ ). The energy separation between the  $X_{\text{CBI-HHI}}$  and the  $\text{Be}^0\text{X}$  is 3.7meV, which is the energy required removing the exciton from the  $\text{Be}^0\text{X}$  complex. The intensity ratio of the  $\text{Be}^0\text{X}$  with the  $X_{\text{CBI-HHI}}$  is 0.76 at 4K and decreases as the measuring temperature increases. As the temperature arrives at 80K, the  $\text{Be}^0\text{X}$  peak is no longer detectable, and the light free exciton peak ( $X_{\text{CBI-LHI}}$ ) can be

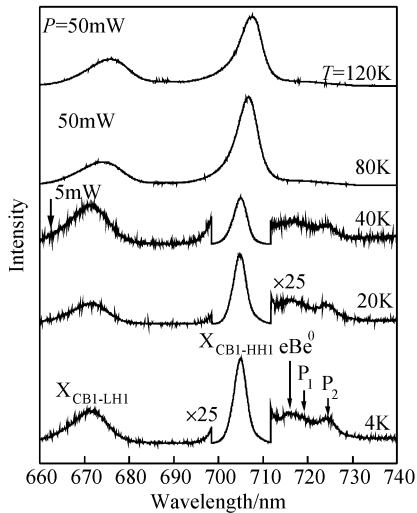


Fig.2 Series of PL spectra of the sample 1 ( $L = 3\text{nm}$ ) at different measuring temperatures with the excitation power of the 514.5nm radiation, showing the  $X_{\text{CBI-LHI}}$ ,  $X_{\text{CBI-HHI}}$ ,  $\text{Be}^0\text{X}$ ,  $\text{eBe}^0$ ,  $P_1$  and  $P_2$  peaks. The excitation is 50mW for the spectra at 80 and 120K.

observed. The third peak at 806.26nm is weaker than the  $X_{\text{CBI-HHI}}$  and  $\text{Be}^0\text{X}$ , which is attributed to the free-to-bound recombination ( $\text{eBe}^0$ ) between an electron of the  $n = 1$  quantized confinement level and a hole bound to a Be acceptor at the center of the GaAs well. As the measuring temperature increases, the  $\text{eBe}^0$  line becomes very weak without any blue shift. This also shows that the signal cannot be due to a donor-acceptor recombination. In addition, Figure 1 shows a weak peak at 1.5324 eV, labeled P, which is interpreted as the two-hole transition (THT) of the Be acceptor bound excitons. The origin of this line is an exciton attached to a neutral Be acceptor. As the exciton recombines, there is a small probability that some of the energy emitted is absorbed by the hole bound to the acceptor, which then undergoes a transition to an excited state leaving the acceptor, binding the exciton in an excited state instead of the ground state. Therefore, the energy separation between the  $\text{Be}^0\text{X}$  and the P peak corresponds to the energy needed to excite the acceptor from its ground state  $1S_{3/2}(\Gamma_6)$  to the first excited state  $2S_{3/2}(\Gamma_6)$ , 25.6meV for this sample. This transition energy is equal to 19.9meV for sample 5, a single GaAs:Be epilayer (as a limiting case with an infinite quantum-well width), in good agreement with what has been reported in Ref. [13]. As the temperature increases, the PL intensities of the  $\text{Be}^0\text{X}$  and P peaks decrease, and the P peak can not be detected at  $T = 20\text{K}$ . The THT is also observed in the other samples in Table 1, but the signal intensity becomes weak as the quantum-well width decreases. This is attributed to a reduction of the free exciton lifetime with a narrower quantum well, and

the probability for the capture by Be acceptors of an electron-hole pair in quantum wells is reduced instead of recombination as a free exciton.

Sample 1 with the well width of 3nm represents the limiting case for doping Be at the center of the GaAs/AlAs multiple quantum wells, and the PL spectra at 4, 20, 40, 80, 120K are given in Fig. 2. In contrast with Fig. 1, there are two distinct features. (1) Only free excitonic peak  $X_{\text{CBI-HHI}}$  has been detected and the bound exciton  $\text{Be}^0\text{X}$  can not be resolved well. It is very weak and probably located at the low-energy side of the asymmetric excitonic signal because above 40K, the excitonic signal shape becomes symmetric. This is mainly due to a reduction of the free exciton lifetime with a narrower QW, and not because of the lower concentration of dopant atoms. The  $\text{Be}^0\text{X}$  is clearly observed in sample 2, which has the same concentration of dopant atoms as sample 1. (2) Figure 2 shows two peaks at wavelengths of 719.10 and 724.27nm, labeled  $P_1$  and  $P_2$  respectively, which are attributed to THTs.  $P_1$  and P in Fig. 1 are shoulder peaks, but the PL intensity of the  $P_1$  peak is much weaker than that of the P peak. As the QW width decreases, the acceptor binding energy increases and the ground state is lowered in energy relative to the excited state, resulting in a reduction in the probability of the two-hole transition occurring<sup>[14]</sup>. The  $P_1$  peak, like P in Fig. 1, is associated with the transition among Be acceptor states,  $1S_{3/2}(\Gamma_6) \rightarrow 2S_{3/2}(\Gamma_6)$ , 31.12meV for sample 1 and the  $P_2$  peak with the transition  $1S_{3/2}(\Gamma_6) \rightarrow 3S_{3/2}(\Gamma_6)$ . This is the narrowest well in the GaAs/AlAs system for which the two-hole transition has been observed.

### 3 Calculation and discussion

#### 3.1 Theory

The Hamiltonian of a beryllium impurity atom within semiconductor GaAs/AlAs multiple quantum wells under the single-band effective mass and envelope function approximations is:

$$H = -\frac{\hbar^2}{2} \times \frac{\partial}{\partial z} \times \frac{1}{m^*} \times \frac{\partial}{\partial z} + V(z) - \frac{e^2}{4\pi\epsilon_0\epsilon_r r} \quad (1)$$

where  $m^*$  is the effective mass of a hole carrier,  $\epsilon_r$  is the relative dielectric permittivity,  $V(z)$  is the one-dimensional electrostatic potential, and  $r$  is the distance between the impurity and the hole carrier. Placing the  $x$  and  $y$  origins on the impurity atom, which is at the position  $r_1$ , then:

$$r^2 = x^2 + y^2 + (z - r_1)^2 \quad (2)$$

The success of variational approaches centers on the general choice of the trial wave function. We choose

the product of two terms as the trial wave function of a hole carrier:

$$\Psi = \Psi(z)\phi(r) \quad (3)$$

where  $\Psi(z)$  is the wave function of the hole in the GaAs/AlAs multiple quantum wells without the acceptor impurity present and  $\phi(r)$  is a hydrogenic-like term describing the interaction between the hole and an acceptor ion.

The hydrogenic factor for the 1s ground state and 2s excited state is taken respectively as:

$$\phi(r) = \exp\left(-\frac{r}{\lambda}\right), \quad \text{for the 1s state} \quad (4)$$

$$\phi(r) = \left(1 - \frac{r}{\lambda}\right)\exp\left(-\frac{r}{\lambda}\right), \quad \text{for the 2s state} \quad (5)$$

where  $\lambda$  is well known as the Bohr radius, but now it is employed as a variational parameter.

The variational calculation is implemented by adjusting  $\lambda$  in order to minimize the expectation value of the Hamiltonian operator, the total energy of the system:

$$E = \frac{\langle \Psi | H | \Psi \rangle}{\langle \Psi | \Psi \rangle} \quad (6)$$

The energy  $E$  is evaluated for different values of  $\lambda$  by direct numerical integration of the numerator and denominator in the above equation.

### 3.2 Results and discussion

In this subsection the numerical results of the energies of the 2s-1s transitions of the Be acceptors at the center of the GaAs/AlAs multiple quantum wells as a function of the well width will be given. We use the formula  $V(z) = 0.33\Delta E_g(x)^{[15]}$ , where  $\Delta E_g(x)$  is the difference in band gaps at  $k = 0$  between GaAs and  $\text{Al}_x\text{Ga}_{1-x}\text{As}$ .  $\Delta E_g(x)$  is taken to be  $1247x$  meV and  $x$  is the mole fraction of the  $\text{Al}_x\text{Ga}_{1-x}\text{As}$  barriers. Although the single-well potential  $V(z)$  makes it more appropriate for completely decoupled quantum wells, it will also be appropriate for multiple quantum wells with thick barriers that no hole wave function can penetrate. The effective mass  $m^*$  is used as the heavy-hole mass of  $0.62m_0$ , the typical value in bulk GaAs, where  $m_0$  is the mass of an electron in the free space. The relative dielectric permittivity,  $\epsilon_r$ , is set to 17.2. In previous theoretical calculations, a great deal of attention has been paid to the roles of the effective mass and the dielectric constant mismatches at interfaces in semiconductor heterostructures, and their effects on the shallow impurity energy levels in the quantum wells<sup>[16~18]</sup>. With  $m^*$  and  $\epsilon_r$  parameters given above, we deduce the acceptor binding energy of 28.0meV for very large well widths, which is in good agreement with the experimental result in bulk GaAs<sup>[6]</sup>. Figure 3 illustrates the theoretical calcula-

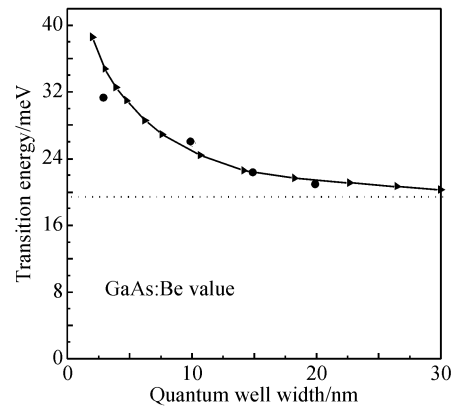


Fig.3 Dependence of the transition energy for the  $1S_{3/2}(\Gamma_6) \rightarrow 2S_{3/2}(\Gamma_6)$  transition for the Be acceptor on the quantum well width, which binds the exciton. The solid circle dots and dot line indicate the experimental data, and the curve with triangle symbols represents the theoretical calculation.

tion results of 2s-1s acceptor transition energies as a function of the quantum-well width for the on-center Be  $\delta$ -doped in GaAs/AlAs multiple-quantum wells according to the above theory. The solid circle symbols and the dotted line in Fig. 3 show experimental data via the PL measurements. The PL experimental measuring results are in good agreement with the theoretical calculation. As the quantum-well thickness increases, the  $1S_{3/2}(\Gamma_6) \rightarrow 2S_{3/2}(\Gamma_6)$  transition energy decreases monotonically, and is close to 19.9meV of the GaAs:Be bulk as the quantum-well thickness is more than 30nm. Compared with Holtz *et al.*'s experimental work on GaAs/ $\text{Al}_{0.3}\text{Ga}_{0.7}\text{As}$  quantum wells with the same quantum-well width<sup>[11]</sup>, the  $1S_{3/2}(\Gamma_6) \rightarrow 2S_{3/2}(\Gamma_6)$  transition energy of the acceptors confined at the centre of the GaAs/AlAs multiple quantum wells is significantly enhanced, but both of them increase as the effect of quantum-well confinement increases. This is mainly due to the confinement effect of quantum wells pushing the hole closer to the negative core, thereby increasing Be acceptor binding energies. Meanwhile, the ground state is lowered in energy relative to the excited states, resulting in an increase in transition energies as the quantum well width decreases. This similar behavior is also observed for shallow donor impurities quantum confined in GaAs/ $\text{Al}_x\text{Ga}_{1-x}\text{As}$  multiple quantum wells<sup>[19]</sup>. As the width of the quantum well decreases, the effect of quantum-well potential confinement for acceptors at the centre of the GaAs/AlAs multiple quantum wells is significantly enhanced. Both the theoretical calculation line and the experimental data of the  $1S_{3/2}(\Gamma_6) \rightarrow 2S_{3/2}(\Gamma_6)$  acceptor transition energies increase monotonically in the same tendency. It is suggested that the acceptors confined in GaAs/AlAs multiple quantum wells can

be described as an ideal hydrogenic atom, and that the single-band effective mass and envelope function approximation are reasonable.

However, because the quantum-well thickness is less than 3 nm, the theoretical calculation line of the 2s-1s acceptor transition energies as a function of the quantum-well width departs gradually from the experimental results measured as the width of the quantum well decreases. This is mainly attributed to two reasons which are not considered in our theoretical model. The first, with the quantum-well potential for acceptor confinement effect increasing, the spin-orbit coupling and the coupling between heavy-hole and light-hole bands should be included in our theoretical calculation. The second, as the quantum-well thickness becomes narrow, the influence of the potential spike resulting from the monolayer of the  $\delta$ -doped acceptors in GaAs/AlAs multiple quantum wells on acceptor states can not be also neglected in calculations. In addition, there are some questions to be investigated further in our theoretical model, for example, the use of the dielectric constant in bulk GaAs has to be employed in the theoretical calculation for the GaAs/AlAs multiple-quantum wells. In the majority of cases, its use is probably fine, however, it is worthwhile noting that there is a change in the permittivity as the effect of the quantum-well confinement on acceptor states enhances and the bound hole approaches to the acceptor.

## 4 Conclusion

In summary, we have investigated both experimentally and theoretically the internal transitions of shallow acceptors confined in GaAs/AlAs multiple-quantum wells. The PL spectra were measured at various temperatures, and two-hole transitions of the acceptor-bound exciton have been observed for a series of Be  $\delta$ -doped GaAs/AlAs multiple-quantum wells and GaAs/Be epilayers. A variational calculation is presented to obtain the 1s-2s acceptor transition energy as a function of a well width. It is found that the acceptor transition energy between the ground state and the first excited state increases monotonically as the quantum-well width decreases, and the experimental data are in good agreement with the theoretical calculation.

## References

- [ 1 ] Liu H C, Song C Y, SpringThorpe A J. Terahertz quantum-well photodetector. *Appl Phys Lett*, 2004, 84: 4068
- [ 2 ] Kundrotas J, Cerskus A, Asmontas S, et al. Excitonic and impurity-related optical transitions in Be  $\delta$ -doped GaAs/AlAs multiple quantum wells: fractional space approach. *Phys Rev B*, 2005, 72: 235322
- [ 3 ] Halsall M P, Harrison P, Wells J P, et al. Picosecond far-infrared studies of intra-acceptor dynamics in bulk GaAs and  $\delta$ -doped AlAs/GaAs quantum wells. *Phys Rev B*, 2001, 63: 155314
- [ 4 ] Zhang Bin, Zhou Shaomin, Wang Haiwei, et al. Raman scattering and photoluminescence of Fe-doped ZnO nanocantilever arrays. *Chin Sci Bull*, 2008, 53: 1639
- [ 5 ] Sze S M. *Physics of semiconductor devices*. New York: John Wiley & Sons, 1981
- [ 6 ] Masselink W T, Chang Y C, Morkoc H. Acceptor spectra of  $\text{Al}_x\text{Ga}_{1-x}\text{As}$ -GaAs quantum wells in external fields: electric, magnetic, and uniaxial stress. *Phys Rev B*, 1985, 32: 5190
- [ 7 ] Gammon D, Merlin R, Masselink W T, et al. Raman spectra of shallow acceptors in quantum-well structures. *Phys Rev B*, 1986, 33: 2919
- [ 8 ] Reeder A A, McCombe B D, Chambers F A, et al. Far-infrared study of confinement effects on acceptors in GaAs/ $\text{Al}_x\text{Ga}_{1-x}\text{As}$  quantum wells. *Phys Rev B*, 1988, 38: 4318
- [ 9 ] Halsall M P, Zheng W M, Harrison P, et al. Binding energy and dynamics of Be acceptor levels in AlAs/GaAs multiple quantum wells. *Journal of Luminescence*, 2004, 108: 181
- [ 10 ] Holtz P O, Sundaram M, Simes R, et al. Spectroscopic study of an acceptor confined in a narrow GaAs/ $\text{Al}_x\text{Ga}_{1-x}\text{As}$  quantum well. *Phys Rev B*, 1989, 39: 13293
- [ 11 ] Kundrotas J, Cerskus A, Asmontas S, et al. Experimental study of optical transitions in Be-doped GaAs/AlAs multiple quantum wells. *Acta Physica Polonica A*, 2005, 107: 245
- [ 12 ] Missous M. Stoichiometric low-temperature GaAs and AlGaAs: A reflection high-energy electron-diffraction study. *J Appl Phys*, 1995, 78: 4467
- [ 13 ] Garcia J C, Beye A C, Contour J P, et al. Reduced carbon acceptor incorporation in GaAs grown by molecular beam epitaxy using dimmer arsenic. *Appl Phys Lett*, 1988, 52: 1596
- [ 14 ] Zheng W M, Halsall M P, Harmer P, et al. Acceptor binding energy in  $\delta$ -doped GaAs/AlAs multiple-quantum wells. *J Appl Phys*, 2002, 92: 6039
- [ 15 ] Harrison P. *Quantum wells, wires and dots: theoretical and computational physics*. England: John Wiley & Sons, 2000
- [ 16 ] Mailhot C, Chang Y C, McGill T C. Energy spectra of donors in GaAs- $\text{Ga}_{1-x}\text{Al}_x\text{As}$  quantum well structures in the effective-mass approximation. *Phys Rev B*, 1982, 26: 4449
- [ 17 ] Fraizzoli S, Bassani F, Buczko R. Shallow donor impurities in GaAs- $\text{Ga}_{1-x}\text{Al}_x\text{As}$  quantum-well structures: role of the dielectric-constant mismatch. *Phys Rev B*, 1990, 41: 5096
- [ 18 ] Oliveira L. Spatially dependent screening calculation of binding energies of hydrogenic impurity states in GaAs- $\text{Ga}_{1-x}\text{Al}_x\text{As}$  quantum wells. *Phys Rev B*, 1988, 38: 10641
- [ 19 ] Jarosik N C, McCombe B D, Shanabrook B V, et al. Binding of shallow donor impurities in quantum-well structures. *Phys Rev Lett*, 1985, 54: 1283

## 量子阱中 Be 受主的光致发光\*

郑卫民<sup>†</sup> 李素梅 吕英波 王爱芳 吴爱玲

(山东大学威海分校 空间科学与物理学院, 威海 264209)

**摘要:** 报道了掺杂在 GaAs 体材料中和  $\delta$  掺杂在一系列 GaAs/AlAs 多量子阱中的 Be 受主带间跃迁的光致发光. 实验所用样品, GaAs 体材料中均匀掺杂 Be 受主的外延单层和一系列量子阱宽度从 3 到 20nm, 并在量子阱中央进行了 Be 受主  $\delta$  掺杂的 GaAs/AlAs 多量子阱样品都是通过分子束外延技术制备的. 在 4, 20, 40, 80 及 120K 不同温度下, 分别对上述样品进行了光致发光谱的测量, 清楚地观察到了受主束缚激子从  $1S_{3/2}(\Gamma_6)$  基态到同种宇称  $2S_{3/2}(\Gamma_6)$  激发态的两空穴跃迁, 并从实验上得到了不同量子阱宽度下 Be 受主从  $1S_{3/2}(\Gamma_6)$  到  $2S_{3/2}(\Gamma_6)$  态的带间跃迁能量. 理论上利用变分原理, 在单带有效质量模型和包络函数近似下, 数值计算了 Be 受主  $1S_{3/2}(\Gamma_6) \rightarrow 2S_{3/2}(\Gamma_6)$  的跃迁能量随量子阱宽度的变化关系, 比较发现理论计算和实验结果符合较好.

**关键词:** 量子限制的受主;  $\delta$  掺杂; 多量子阱; 光致发光

**PACC:** 7320D; 7855E; 7155F

**中图分类号:** TN304.2<sup>+</sup>3

**文献标识码:** A

**文章编号:** 0253-4177(2008)11-2115-06

\* 国家自然科学基金(批准号:60776044)及山东省自然科学基金(批准号:2006ZRA10001)资助项目

<sup>†</sup> 通信作者. Email:wmzheng@sdu.edu.cn

2008-06-03 收到, 2008-07-15 定稿